

VALIDATION OF COMPUTATIONAL FLUID DYNAMIC ANALYSIS OF NATURAL CONVECTION CONDITIONS FOR A RESIN DRY-TYPE TRANSFORMER WITH A CABIN

by

Gulsen YAMAN^{a*}, Ramazan ALTAY^b, and Ramazan YAMAN^c

^a Department of Mechanical Engineering, Balikesir University, Balikesir, Turkey

^b BEST A. S., R&D Department, Balikesir, Turkey

^c Department of Industrial Engineering, Gelisim University, Istanbul, Turkey

Original scientific paper

<https://doi.org/10.2298/TSCI180919327Y>

Many industrial products work under different constraints. Examples of these products include transformers and keeping them in certain operating temperatures is an important design constraint. However, since power transformers have different requirements, there are no standard products. For this reason, it is difficult and costly to test each one by considering these constraints and to design them accordingly. Satisfactory thermal analysis using a 3-D finite volume-based CFD model is an important step to understand natural convection and necessary design modifications under the desired conditions.

The aim of this study is to verify the performance and reliability of the design by comparing the experimental results with 3-D finite volume analysis results by considering cooling of a dry resin type transformer with a cabin. The effect of the cabin on the product in terms of natural heat convection is also evaluated.

Key words: CFD analysis, natural heat convection, dry-type transformer, temperature distribution

Introduction

A transformer is an electrical device that transfers electrical energy between two or more circuits through electromagnetic induction without changing the frequency and has no moving parts. Transformers can be classified in two main groups as dry-type (in ambient air) and oil-filled type in terms of insulation and cooling systems. Dry-type transformers are cooled by two basic heat transfer methods: air natural convection and air natural-air forced convection. Dry-type transformers are manufactured with cabins according to desired International Protection Marking standards (in this study, this is IP-31).

Convection is heat transfer due to bulk movement of molecules within fluids such as gases and liquids. Natural cooling is the result of decreasing density of heated air and movement in the opposite direction to gravity. This movement results in air reaching a certain velocity causing heat transfer by convection through the contact surfaces. As a result of this, the transformer is naturally cooled. Natural cooling is enhanced by leaving ventilation holes in the upper and lower parts of the cabin. The air that enters the bottom ventilation holes at ambient temperature heats up because of the energy loss of the transformer. The heated air moves to-

* Corresponding author, e-mail: yamangulsen@gmail.com

wards the upper ventilation holes. While this cycle of movement goes on continuously, cooling of the transformer is ensured as a matter of course.

Designs of dry-type transformers are regulated by the standard IEC 70016-11. Ambient temperature values must be known in order to calculate the desired winding temperatures. It is not correct to assume that the temperature inside the cabin and the ambient temperature are equal for dry-type transformers. For this reason, determining the effect of the cabin geometry on the transformer's core temperature and choosing the most effective cabin geometry for optimum cooling performance is very important.

Literature review

Much research has been carried out on prediction of heat generation in the coils, and how the heat is distributed between them. Reviewed research articles that mention these matters can be presented in the following manner when briefly evaluated in terms of their main context.

Komurgoz and Guzelbeyoglu [1] analyzed the temperature distributions of the coils and core obtained by finite element method considering the cooling effect of the oil channels between the windings and the core. As well as the temperature distribution in the windings and the core, temperature distribution and movement of the surrounding air was also determined. The temperature level and the location of the hot spots were determined. The effect of air ducts on the coil temperature in constant and varying ambient conditions in dry-type transformers for different powers was analyzed by Lee *et al.* [2] who also compared calculated temperature values with the experimentally-measured temperature values.

Rahimpour and Azizian [3], and Eslamian *et al.* [4] investigated the effect of temperature variations on the coils with different numbers of air ducts in dry-type transformers. The effect of eddy losses and radiation on the temperature of the coil was also investigated. Moreover, it was proven that the paper bands used in coils have no effect on temperatures [3]. Dry-type transformers were investigated by Eteiba *et al.* [5] in terms of the temperature distributions of coils and cores at different ambient temperatures. The effect of air ducts with different dimensions on the temperatures of windings was also investigated.

A thermal model of the oil-filled-type transformer for oil natural convection cooling system was created and the determined values were compared with the test results from an identical transformer by Gastelarrutia *et al.* [6]. The temperatures and velocity distributions obtained from the calculations are visually specified in the sections taken from the transformer model. Cremasco *et al.* [7] studied the heat and flow analysis of a dry-type transformer, which was cooled by means of a fan in a cabinet. The CFD and thermal/pressure network models were used in the analysis and the results were compared. As a result of these obtained values, the aim was to optimize the cooling systems.

In 1994, Pierce [8] studied ventilated dry-type transformers and found that hottest spot allowances in IEEE standards for transformers larger than 500 kVA are too low and should be revised. He also developed a mathematical model to predict hottest spot temperature rises in ventilated dry-type transformers. Pierce [8] used a system of finite difference nodal equations to estimate hottest spot temperatures and revised the model using six layer test windings and a 2500 kVA prototype transformer.

Tripathi *et al.* [9] have obtained the temperature distributions of air in the room because of changing the input speeds and room dimensions (aspect ratio) for a closed room. Reynolds number and Gr/Re^2 numbers were modified for three different aspect ratios for the room and as a result the streamline and isotherm charts of the room were obtained.

Hannun *et al.* [10] have studied to increase the cooling performance of a 250 kVA oil-type transformer by means of the earth-air heat exchanger (EAHE) method. Here, the EAHE method was compared with the results of the study using the previously made nanofluid and pure oil. As a result of this study, it was seen that the EAHE method provides more efficient cooling. Also, the pipe diameters and air inlet velocities used in EAHE method were investigated to see the effect of transformer on cooling performance.

Materials and method

This phase can be evaluated in the following stages:

- Deciding on the basis of the model.
- Designing solution steps for the model.
- Solving the model using suitable software.
- Experimental set-up modeling from real system considerations.
- Manufacturing of the experimental set-up.
- Carrying out experiments.
- Collection of the experimental results.
- Comparing and representing the analytical and empirical results.

Mathematical model

The mathematical model for the thermal analysis of a cast resin dry-type transformer was developed to obtain the temperature distribution in the cabin. Some mechanical parts, such as clamps and bolts, were ignored in the model for simplification of the model and experimental set-up.

The structure of a transformer is complex, and some assumptions are required. For the aspect of heat analysis, four main components of the transformer can be considered: iron core, low voltage coils, high voltage coils, and air ducts. With this simplified structure, heat transfer fundamentals can be assessed as follows.

Accordingly, the general equations for the temperature distribution and fluid motion in the transformer are shown below. Equations are derived from the conservation laws in steady-state 3-D [11, 12]:

- mass conservation equation

$$\frac{\partial(\rho u)}{\partial x} + \frac{\partial(\rho v)}{\partial y} + \frac{\partial(\rho w)}{\partial z} = 0 \quad (1)$$

- momentum conservation equation

$$\rho \left(u \frac{\partial u}{\partial x} + v \frac{\partial u}{\partial y} + w \frac{\partial u}{\partial z} \right) = -\frac{\partial p}{\partial x} + \mu \left(\frac{\partial^2 u}{\partial x^2} + \frac{\partial^2 u}{\partial y^2} + \frac{\partial^2 u}{\partial z^2} \right) + S_x \quad (2a)$$

$$\rho \left(u \frac{\partial v}{\partial x} + v \frac{\partial v}{\partial y} + w \frac{\partial v}{\partial z} \right) = -\frac{\partial p}{\partial y} + \mu \left(\frac{\partial^2 v}{\partial x^2} + \frac{\partial^2 v}{\partial y^2} + \frac{\partial^2 v}{\partial z^2} \right) + S_y \quad (2b)$$

$$\rho \left(u \frac{\partial w}{\partial x} + v \frac{\partial w}{\partial y} + w \frac{\partial w}{\partial z} \right) = -\frac{\partial p}{\partial z} + \mu \left(\frac{\partial^2 w}{\partial x^2} + \frac{\partial^2 w}{\partial y^2} + \frac{\partial^2 w}{\partial z^2} \right) + S_z \quad (2c)$$

- energy conservation equation

$$\rho c \left(u \frac{\partial T}{\partial x} + v \frac{\partial T}{\partial y} + w \frac{\partial T}{\partial z} \right) = k \left(\frac{\partial^2 T}{\partial x^2} + \frac{\partial^2 T}{\partial y^2} + \frac{\partial^2 T}{\partial z^2} \right) + q^* + \phi \quad (3)$$

where T [K] represents the temperature, p [Nm^{-2}] – the pressure, q^* [Wm^{-3}] – the heat source, k [$\text{Wm}^{-1}\text{K}^{-1}$] – the thermal conductivity, ρ [kgm^{-3}] – the density of material, c [$\text{Jkg}^{-1}\text{K}^{-1}$] – the specific heat, and μ [$\text{kgm}^{-1}\text{s}^{-1}$] – the dynamic viscosity of fluid. Also, u , v , w are the velocity components in x-, y-, and z-directions. The S_x , S_y , S_z are the mass forces per unit volume in x-, y-, and z-directions, respectively. The ϕ is the viscous dissipation defined:

$$\phi = \mu \left\{ 2 \left[\left(\frac{\partial u}{\partial x} \right)^2 + \left(\frac{\partial v}{\partial y} \right)^2 + \left(\frac{\partial w}{\partial z} \right)^2 \right] + \left(\frac{\partial v}{\partial x} + \frac{\partial u}{\partial y} \right)^2 + \left(\frac{\partial w}{\partial y} + \frac{\partial v}{\partial z} \right)^2 + \left(\frac{\partial u}{\partial z} + \frac{\partial w}{\partial x} \right)^2 \right\} \quad (4)$$

The numerical simulation of heat transfer was carried out with ANSYS 14.5. A 3-D view of a three-phase cast resin dry-type transformer is used in the analysis [13].

To solve conservation equations, many boundary conditions must be applied to the surfaces of the model. Winding losses, convection and radiation relations are used to obtain a complete graph of the temperatures at every location in the model. In natural convection problem solutions, temperature and velocity of fluid are interdependent, so all basic equations are iteratively and simultaneously solved. From the solution of the equations, it is possible to determine the heat transfer coefficients between the surfaces and the fluid, to obtain the flow fields and to find the temperature fields of the whole system as solids and fluids.

Natural convection: The heat transfer rate of convection is obtained using the equation below [12]:

$$q''_{\text{conv}} = h(T_s - T_{\text{air}}) \quad (5)$$

where q''_{conv} [Wm^{-2}] represents heat transfer rate per unit area at the outer surface, h [$\text{Wm}^{-2}\text{K}^{-1}$] – the heat transfer coefficient for convection from outer surface, T_s [K] – the local temperature of surface, and T_{air} [K] – the ambient temperature.

The theoretical equations for convective heat transfer are quite complex [11, 12]. The resulting transport equations are usually experimentally-obtained formulations. These formulations are not essential here. The main equations used in the natural convection heat transfer are as follows:

Heat transfer coefficient, h :

$$h = \frac{\text{Nu} k_{\text{air}}}{L_c} \quad (6)$$

Grashoff, Rayleigh, and Prandtl numbers:

$$\text{Gr}_L = \frac{g \beta (T_s - T_{\text{air}}) L_c^3}{\nu^2} \quad \text{Ra}_L = \text{Gr}_L \text{Pr} \quad \text{Pr} = \frac{c \mu}{k_{\text{air}}} \quad (7)$$

where g [ms^{-2}] represents acceleration of gravity, β [K^{-1}] – the volumetric expansion of fluid, ν [m^2s^{-1}] – the kinematic viscosity of fluid, μ [$\text{kgm}^{-1}\text{s}^{-1}$] – the dynamic viscosity of fluid, c [$\text{Jkg}^{-1}\text{K}^{-1}$] – the specific heat, and L_c [m] – the characteristic length of geometry.

Radiation: Outer surface is a vertical cylindrical surface and can be assumed as a vertical plate. Two types of heat transfer can occur on the outer surface, including radiation and natural convection.

For the outer surface, radiation can be expressed using the equations [11, 12]:

$$q_r'' = \varepsilon\sigma(T_s^4 + T_{\text{air}}^4) = h_r(T_s - T_{\text{air}}) \quad (8)$$

$$h_r = \sigma\varepsilon(T_s + T_{\text{air}})(T_s^2 + T_{\text{air}}^2) \quad (9)$$

where q_r'' [Wm^{-2}] – the heat transfer rate per unit area by radiation, h_r [$\text{Wm}^{-2}\text{K}^{-1}$] – the local heat transfer coefficient for radiation from outer surface, and ε is emissivity coefficient of surface. Also, T_s [K] – the local temperature of the surface, T_{air} [K] – the ambient temperature, and $\sigma = 5.67 \cdot 10^{-8} \text{ W/m}^2\text{K}^4$ is Stephan Boltzmann's coefficient.

The CFD analysis using FLUENT

In the analysis, firstly a 3-D model of the internal volume which is the gas for the fluid analysis is created. For creation of this model, designed solid volumes were subtracted from the total volume of the cabin rather than the volume defining the boundary conditions. AUTODESK INVENTOR software was used for all these stages, see fig. 1.

The created 3-D mesh structure is presented in fig. 2. The mesh structure plays an important role in the calculations. The mesh elements are volume and they are defined and placed semi-automatically by the ANSYS/FLUENT software. The mesh structure of the problem is prepared using the *curvature size* function. Mesh structure is mostly composed of *tetrahedral mesh*. A total of 7293011 elements and 1599753 points are used in the model. Figure 3 shows temperature distribution in the cabin. Knowing these distribution and temperature values are important before manufacturing the transformer and its cabin. These predicted parameters improve the design and shortened the test times.

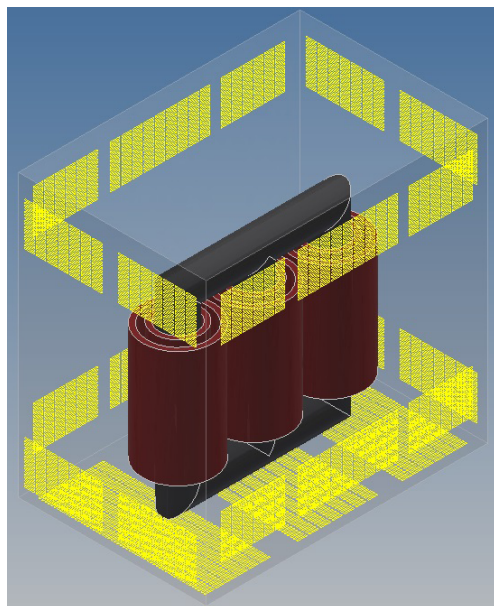


Figure 1. The 3-D Model of the transformer for the ANSYS Fluent Analysis (Prepared fluid flow volume)

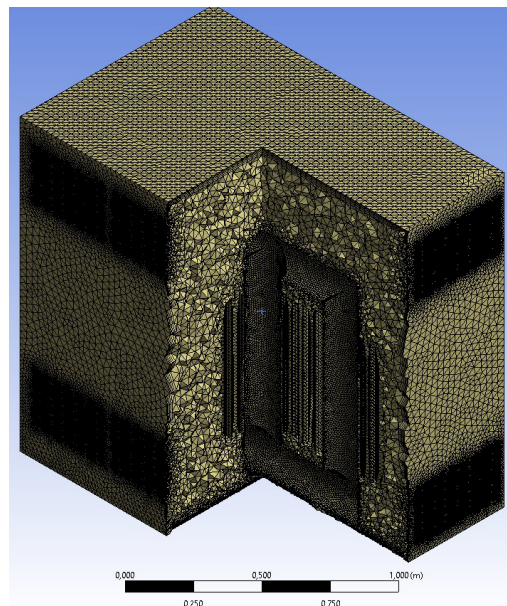


Figure 2. Mesh structure of the 3-D model for Fluent analysis

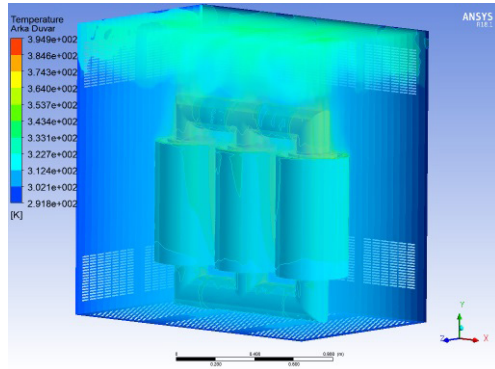


Figure 3. Temperature distribution of 3-D model (for color image see journal web site)

In this regard, FLUENT (ANSYS) was chosen among possible software programs as it is proven to be successful and accepted. Then, the values of these boundary surfaces were determined and entered into the program for the analysis. When entering the limit surface, the measured values of a similar previously-manufactured transformer are used (250 kVA 11/0.4 kV Dyn11 BEST dry-type transformer).

Following the construction of this model design and determination of the requirements for the CFD analysis, the following sample forms for gradients of internal volume air temperatures, figs. 4(a) and 4(b), were observed.

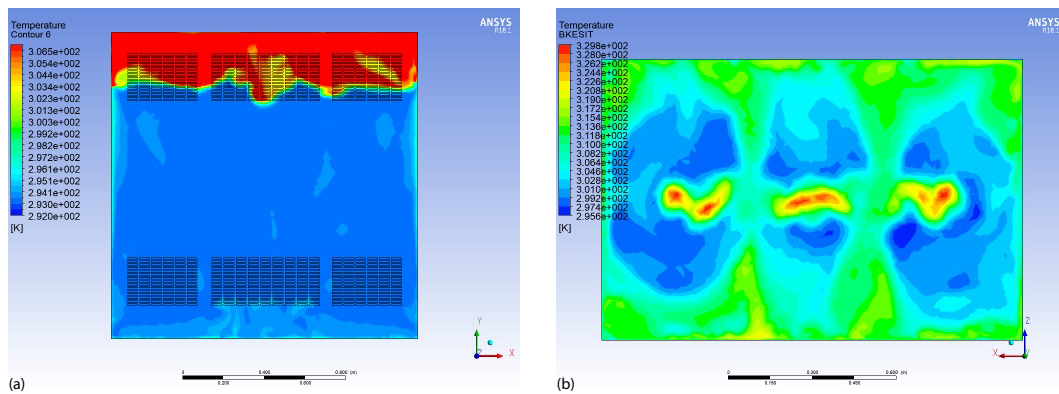


Figure 4. (a) Cross-section (X-Y) analysis of the prepared model, (b) cross-section (X-Z) analysis of the prepared model (for color image see journal web site)

Experimental set-up

In order to verify the success of the model, a real cabin was prepared by considering the actual transformer dimensions and design. For design and construction of the experimental set-up, measurements are intended to be made easily and to form the closest values to the true temperatures. It is assumed that most of the losses that occur here (eddy losses and noise losses are neglected) are converted to heat. Three quartz resistances (each 1 kW) were used to represent the cores and they were placed in the specially-designed cylindrical volumes. These cylindrical volumes also have the actual dimensions of the winding volume and are shaped with suitable geometries to allow heat flow in the upper and lower cores.

Figures 5(a) and 5(b) shows the cross-section (X-Z) and (X-Y) of the internal structure of the prepared model, respectively.

Thermocouple sensors were also attached to the tensioned 0.3 mm diameter wires that were connected to the co-ordinates of the specified points to form each measurement range, and the measurements continued every 30 seconds until the system temperature values became stable. The appearance of the data collection devices (HOBO data logger) and thermocouples is shown in figs. 6 and 7.

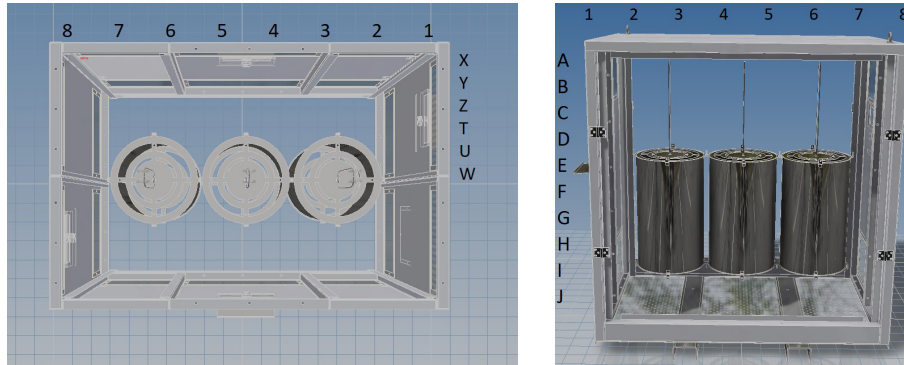


Figure 5. A view of the internal structure of the prepared model (a) in (X-Z) direction and (b) in (X-Y) direction



Figure 6. Data collection devices and test set view during measurements



Figure 7. The view of the location of the thermocouples during measurements

Numerical analysis and experimental results

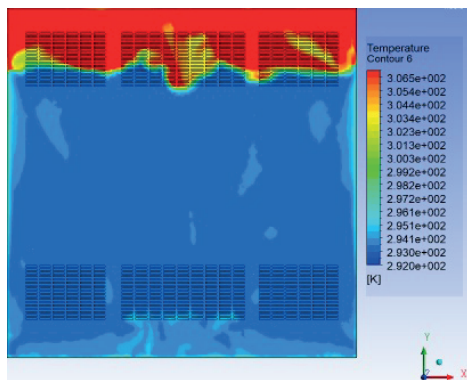
For certain co-ordinates, the experimental values and numerical values could be compared with fig. 8 and tab. 1. This comparison verifies the thermal model and its analysis. So, these verifications indicate that design and manufacturing of the system can be supported and improved with the CFD analysis.

Table 1. Some temperatures values for comparison

A	X		Y		Z	
	CFD	Exp.	CFD	Exp.	CFD	Exp.
1	34.95	31.83	39.63	37.84	35.97	37.96
2	34.25	34.65	37.32	37.46	34.25	36.30
3	37.39	35.71	38.76	38.52	37.88	37.16
4	37.32	35.82	39.69	39.50	38.14	38.28
5	36.78	35.38	37.10	38.52	37.76	38.00
6	38.50	34.73	38.29	38.41	37.90	37.47
7	34.51	33.99	37.51	37.03	34.30	35.50
8	33.33	31.96	39.90	37.68	35.44	36.64

	1	2	3	4	5	6	7	8														
A	31.830	32.770	33.710	34.650	35.590	36.530	37.470	38.410	39.350	40.290	41.230	42.170	43.110	44.050	44.990	45.930	46.870	47.810	48.750			
B	33.760	33.703	33.647	33.590	34.070	34.550	35.030	35.510	36.440	36.920	37.400	37.880	38.360	39.290	39.770	40.250	40.730	41.660	42.140	42.620		
C	32.15	31.240	30.330	29.42	30.663	31.907	33.151	33.243	33.337	33.43	33.593	33.757	33.92	33.910	33.900	33.89	32.710	31.530	30.35	30.827	31.303	31.78
D	24.11	24.127	24.143	24.16	24.670	25.180	25.69	25.777	25.263	25.05	24.993	24.937	24.88	25.617	26.353	27.09	26.470	25.850	25.23	25.143	25.057	24.97
E	24.68	24.713	24.747	24.78	25.023	25.267	25.51	25.397	25.283	25.17	25.200	25.230	25.26	25.197	25.133	25.07	24.980	24.890	24.8	24.580	24.360	24.14
F	23.88	23.900	23.920	23.94	24.263	24.587	24.91	24.817	24.723	24.63	24.790	24.950	25.11	24.900	24.690	24.48	24.357	24.233	24.11	23.953	23.797	23.64
G	23.95	23.913	23.877	23.84	23.917	23.993	24.07	24.387	24.703	25.02	24.907	24.793	24.68	24.780	24.880	24.98	24.780	24.580	24.38	23.977	23.573	23.17
H	26.41	26.410	26.410	26.41	26.337	26.263	26.19	26.483	26.777	27.07	26.887	26.703	26.52	26.543	26.567	26.59	26.513	26.437	26.36	26.100	25.840	25.58
I	26.4	26.493	26.587	26.68	26.860	27.040	27.22	27.407	27.593	27.78	27.790	27.680	27.63	27.603	27.577	27.55	27.327	27.103	26.88	26.777	26.673	26.57
J	25.71	25.650	25.590	25.53	26.377	27.223	28.07	27.447	26.823	26.2	26.223	26.247	26.27	26.147	26.023	25.9	25.663	25.427	25.19	25.460	25.730	26

(a)



(b)

Figure 8. Comparison of test results and CFD analysis
 Z = 0.45 m (X cross-section)
 (for color image see journal web site)

This study has shown that when the CFD analysis and the experiments can be performed correctly, the results can be taken into consideration and used for design and improvements. However, in order to be able to test each cabin according to the experiment, approximately 480 ($6 \times 10 \times 8$) points were measured in spite of symmetry acceptance. This was completed with 60 measurements. Approximately 45 minutes of measurement

time was required excluding preparations for each measurement. This indicates the cost of time and labor.

Conclusions and further studies

As a result of this CFD analysis and experimental work, the variation of temperature distributions in the cabin was determined for a dry-type transformer with cabin. The obtained CFD analysis data and the experimental data comply with each other. It offers important indications that CFD analysis can be a significant contributor to transformer cabin design with new dimensions and specifications and may be a decisive step in decision-making. Thus, cabin design can be completed in a shorter time, and only with the last analysis. In addition, studies may be recommended for further work to ensure a more efficient natural flow by modifying the design and geometry of the cabin (cabin roof, air inlet and outlet locations).

Acknowledgment

We would like to thanks BEST A. S. for support in completing the experimental work.

Nomenclature

c	– specific heat, [Jkg ⁻¹ K ⁻¹]
g	– acceleration of gravity, [ms ⁻²]
h	– heat transfer coefficient for convection from outer surface, [Wm ⁻² K ⁻¹]
h_r	– local heat transfer coefficient for radiation from outer surface, [Wm ⁻¹ K ⁻¹]
k	– thermal conductivity, [Wm ⁻¹ K ⁻¹]
L_c	– characteristic length of geometry, [m]
q	– heat transfer rate per unit area at the outer surface, [Wm ⁻²]
q^*	– heat source, [Wm ⁻³]
S_x, S_y, S_z	– mass forces per unit volume in x-, y-, z-directions
T	– temperature, [K]
T_{air}	– ambient temperature, [K]
T_s	– local temperature of surface, [K]
u, v, w	– velocity components in x-, y-, z-directions

Greek symbols

β	– volumetric expansion of fluid, [K ⁻¹]
μ	– dynamic viscosity of fluid, [kgm ⁻¹ s ⁻¹]
$\mu\phi$	– viscous dissipation
ε	– emissivity coefficient of surface
ν	– kinematic viscosity of fluid, [m ² s ⁻¹]
ρ	– density, [kgm ⁻³]
σ	– Stephan Boltzmann's coefficient, (= 5.67·10 ⁻⁸ W/m ² K ⁴)

Subscripts

air	– ambient (air)
c	– characteristic
r	– radiation
s	– surface
x, y, z	– Cartesian co-ordinates

References

- [1] Komurgoz, G., Guzelbeyoglu, N., Determining of the Temperature Distribution of Self-Cooled Dry Type Power Transformers, *Iju Journal/d, Engineering*, 1 (2002), 1
- [2] Lee, M., *et al.*, Air Temperature Effect on Thermal Models for Ventilated Dry-Type Transformers, *Electric Power Systems Research*, 81 (2011), 3, pp. 783-789
- [3] Rahimpour, E., Azizian D., Analysis of Temperature Distribution in Cast-Resin Dry-Type Transformers, *Electrical Engineering*, 89 (2007), 4, pp. 301-309
- [4] Eslamian, M., *et al.*, Thermal Analysis of Cast-Resin Dry-Type Transformers, *Energy Conversion and Management*, 52 (2011), 7, pp. 2479-2488
- [5] Eteiba, M. B., *et al.*, Steady State Temperature Distribution of Cast-Resin Dry Type Transformer Based on New Thermal Model Using Finite Element Method, *World Academy of Science, Engineering and Technology*, 4 (2010), 2, pp. 806-810
- [6] Gastelurrutia, J., *et al.*, Numerical Modelling of Natural Convection of Oil Inside Distribution Transformers, *Applied Thermal Engineering*, 31 (2011), 4, pp. 493-505
- [7] Cremasco, A., *et al.*, Thermal Simulations for Optimization of Dry Transformers Cooling System, *Scientific Computing in Electrical Engineering, Mathematics in Industry*, 23 (2016), Jan., pp. 103-113
- [8] Pierce, L. W., Predicting Hottest Spot Temperatures in Ventilated Dry Type Transformer Windings, *IEEE Transactions on Power Delivery*, 9 (1994), 2, pp. 1160-1172

- [9] Tripathi, B., *et al.*, A CFD Analysis of Room Aspect Ratio on the Effect of Buoyancy and Room Air Flow, *Thermal Science*, 11 (2007), 4, pp. 79-94
- [10] Hannun, R. M., *et al.*, Heat Transfer Enhancement from Power Transformer Immersed in Oil by Earth Air Heat Exchanger, *Thermal Science*, On-line first, <https://doi.org/10.2298/TSCI117231116H>
- [11] Holman, J. P., *Heat Transfer*, McGraw-Hill Book Company, New York, USA, 2014
- [12] Incropera, F. P., David, P. D., *Fundamentals of Heat and Mass Transfer*, John Wiley and Sons, New York, USA, 2011
- [13] ***, ANSYS R14.5, FLUENT in ANSYS Workbench User's Guide, 2012